Type of the Paper (Article)

Alteration of retinal metabolism and oxidative stress may implicate myopic eye growth: evidence from discovery and targeted proteomics in an animal model

Feng-Juan Yu[a,1], Thomas Chuen Lam[a,1*], Andes Ying-Hon Sze[a], King-Kit Li[a], Rachel Ka-Man Chun[a], Sze-Wan Shan[a] and Chi-Ho To[a]

[a] Laboratory of Experimental Optometry, Centre for Myopia Research, School of Optometry, The Hong Kong Polytechnic University, Hung Hom, Kowloon, Hong Kong

[*] Correspondence: thomas.c.lam@polyu.edu.hk; Tel. : (852)-27666115

[1] These authors contributed equally to this manuscript and are thus considered co-first authors.

Abstract: Myopia, the most common cause of impaired vision, may induce sight-threatening diseases or ocular complications due to axial elongation. The exact

31 mechanisms underlying myopia development have received much attention and

32 understanding of these is necessary for clinical prevention or therapeutics. In this

33 study, quantitative proteomics using Isotope Coded Protein Label (ICPL) was applied

34 to identify differentially regulated proteins in the retinas of myopic chicks and, from

35 their presence, infer the possible pathogenesis of excessive ocular elongation. Newly

36 hatched white leghorn chicks (n = 15) wore -10D and +10D lenses bilaterally for 3

37 and 7 days, respectively, to develop progressive lens-induced myopia (LIM) and

38 hyperopia (LIH). Retinal proteins were quantified with nano-liquid chromatography

39 electrospray ionization coupled with tandem mass spectrometry

40 (nanoLC-ESI-MS/MS). Bioinformatics analysis of differentially regulated proteins

41 revealed that the majority originated from the cytoplasmic region and were related to

42 various metabolic, glycolytic, or oxidative processes. The fold changes of four

43 proteins of interest (vimentin, apolipoprotein A1, interphotoreceptor retinoid binding

44 protein, and glutathione S-transferase) were further confirmed by a novel

45 high-resolution multiple reaction monitoring mass spectrometry (MRM-HR) using a

46 label-free approach.

47 **Significance:** Discovery of effective protein biomarkers of myopia has been

48 extensively studied to inhibit myopia progression. This study first applied

49 lens-induced hyperopia and myopia in the same chick to maximize the inter-ocular

50 differences, aiming to discover more protein biomarker candidates. The findings

51 provided new evidence that myopia was metabolism related, accompanied by altered

52 energy generation and oxidative stress at retinal protein levels. The results in the

53 retina were also compared to our previous study in vitreous using ICPL quantitative

54 technology. We have now presented the protein changes in these two adjacent tissues,

55 which may provide extra information of protein changes during ocular growth in

56 myopia.

1. Introduction

Myopia (nearsightedness), the most common type of refractive error, is accompanied by excessive ocular length. High myopia is frequently associated with ocular complications, including cataract, glaucoma, retinal detachment, and optic disc abnormalities, resulting in higher risks of visual impairment and even blindness [1]. The prevalence of myopia has dramatically increased, although there are variations between regions and ethnic groups. It has been estimated that nearly half of the world's population (5 billion) will become myopic by 2050, of whom 9.8% would suffer from high myopia [2]. The problem is even more severe among young people in urbanized East Asian countries [3-5]. However, the mechanism resulting in myopia onset and progression remains uncertain, limiting the development of therapeutics and effective control of myopia.

The eye undergoes a natural homeostatic emmetropization process during normal growth [6]. Any disturbance to the process from external visual input during the sensitive period may lead to the onset of ametropia. Although there are differences in ocular structures between animals and humans, animal models with active emmetropization are still predominantly used to study myopia [7]. Through the manipulation of experimentally induced ametropic models in different animal species, growth-guiding signal transduction (GO and STOP signals) or molecular targets (gene and protein) during this dynamic balancing process may be identified. Timely activation of STOP signals or deactivation of GO signals may achieve the ultimate goal of controlling de-regulated ocular growth and myopia progression [8].

The retina, the sensory tissue receiving visual inputs, plays a vital role during

83 normal ocular growth and myopia development. It becomes significantly thinner

84 during myopia development [9] and is even considered by some researchers as the

85 origin of myopia onset [10]. Consequently, GO or STOP signals of protein biomarkers

86 in retinal tissue are likely to be critical in myopia prevention. Therefore, many studies

87 using various approaches, including genome-wide association, transcriptome and

88 proteomics techniques have mainly concentrated on the retina [11, 12]. In recent years,

89 proteomic analysis has suggested several protein targets and myopia-associated

90 pathways related to myopia. Among these protein biomarkers, Apolipoprotein A1

91 (Apo A1), originally suggested by proteomics, has been frequently reported as a novel

92 biomarker in ocular tissues, including the retina, choroid, sclera, and vitreous humor

93 [9, 13-15], possibly via participation in regulatory feedback of retinoic acid. Using

94 bioinformatics tools, metabolism and related TGF-beta have also been strongly

95 suggested to have a possible relationship with myopia among other reported gene or

96 protein candidates [14, 16-19]. However, a complete picture of the pathophysiology

97 of myopia has yet to be defined in animal studies.

98   As the retina and vitreous are adjacent tissues, abnormalities of this

99 vitreous-retina complex may be related to vision impairment, including retinal

100 detachment, posterior vitreous detachment, and vitreomacular traction [20]. Based on

101 our recent identification of proteins in the vitreous of normally raised 7-day old chicks

102 and protein quantification in relative myopic chick models using a bilateral LIM and

103 LIH model [19], a similar quantitative proteomic approach was utilized in the present

104 study to identify proteins in the retinal tissue from the same experimental setup in

105 order to investigate potential protein regulation in LIM and LIH chicks. By studying

106 protein changes in these two adjacent tissues, it is expected that a more

107 comprehensive understanding of the mechanisms of myopia progression may be

108 achieved.

2. Materials and Methods

2.1. Animal model

White Leghorn chicks (*Gallus domesticus*) bred from Specific Pathogen-Free eggs (Jinan Spafas Poultry Co, Jinan, China) were housed in stainless steel brooders under a 12-hour light/dark cycle. They received water and food *ad libitum*. All processing procedures, including chick-rearing, handling, and tissue extraction were performed at the animal center of the Hong Kong Polytechnic University and were in compliance with the ARVO statement on the Use of Animals in Research. All experimental procedures performed were also approved by the Animal Subjects Research Ethics Subcommittee of the Hong Kong Polytechnic University in accordance with relevant guidelines and regulations set forth by the Hong Kong Government.

The animal model and measuring procedures in this study were as previously reported [19]. Briefly, chicks aged 4 to 5 days (d0) were mounted with -10D lenses (right eye) and +10D lenses (left eye) for 3 days and 7 days, respectively. There was no gender preference for the experimental chicks. Lenses were made of polymethylmethacrylate with a base curve of 6.7 mm and optical zone diameter of 11.0 mm. Refractive error and ocular dimensions of each eye were measured to assess the speed of ocular growth at different ocular components at various time points. Ocular biometrics, including anterior chamber depth (ACD), lens thickness, vitreous chamber depth (VCD), retina thickness, and choroidal thickness were measured using a high-frequency A-scan ultrasound transducer (Panametrics, Inc., Waltham, MA) at each time point. Refractive status was measured using a Streak retinoscope. The resultant spherical equivalent (S.E. = spherical power + 1/2 cylindrical power) was calculated to express the refractive error.

2.2. Retinal protein extraction

135   After measurement at d3 and d7, chicks were euthanized by carbon dioxide

136   overdose. The eyeball was hemisected equatorially. The vitreous body was discarded,

137   and the optic nerve cut off. The retinal tissue was carefully peeled off from the retinal

138   pigment epithelium and added to 250µL lysis buffer containing 7M urea, 2M thiourea,

139   30mM Tris, 2% (w/v) CHAPS and 1% (w/v) ASB14 in protease inhibitor cocktail

140   (Roche Applied Science, Basel, Switzerland). The mixture was homogenized for 5

141   minutes, using a Teflon freezer mill cooled in liquid nitrogen (Mikro-Dismembrator

142   Braun Biotech, Melsungen, Germany). The closed chamber was then incubated for

143   15-20 minutes at room temperature. The lysate in the chamber was collected and

144   centrifuged at $16.1 \times 1,000$ g for 30 minutes at 4°C. The supernatant was collected for

145   total protein concentration measurement using 2-D Quant Kit (GE Healthcare Life

146   Science, Marlborough, MA).

147   *2.3. Sample pooling and protein digestion for LC-MS/MS*

148   At each d3 and d7 time point, a total of 15 chicks were randomly assigned into

149   groups of five to form three biological replicates. Based on protein concentration,

150   25µg retinal proteins from the right and left eyes of five individual chicks from each

151   group were pooled together to form representative LIM and LIH lysates. The mixtures

152   were then precipitated with ice-cold acetone overnight and the protein pellets

153   reconstituted with guanidine-HCl buffer (6M, pH = 8.5). The protein concentration of

154   each recovered sample was measured again by 2D quant kit, and, subsequently, equal

155   amounts of proteins (100µg for each group) were labeled using an Isotope Coded

156   Protein Labeling kit (ICPL Serva Kit, Germany), according to the manufacturer's

157   instructions. Briefly, proteins in the two samples were differentially labeled with ^{12}C

158   and ^{13}C isotope tags. Then they were combined together, and the proteins

159   subsequently precipitated. The resulting protein pellet was finally reconstituted with

160   1M urea in 25mM ammonium bicarbonate (NH_4HCO_3). Protein mixtures were

161 separated in a mini 1D SDS-PAGE (8% stacking gel and 12% resolving gel). After

162 staining with Coomassie G250 (Sigma-Aldrich, France), the pellet was cut manually

163 into 40 fractions of similar width. Each fraction was reduced (50mM dithiothreitol in

164 25mM NH_4HCO_3), alkylated (100mM iodoacetamide in 25mM NH_4HCO_3), and

165 digested by trypsin (20ng/µL, 10µL). Samples were rehydrated on ice for 30 minutes

166 and further incubated at 37°C overnight (16-18 hours) with gentle shaking.

167 Endo-GluC in 25mM NH_4HCO_3 (33ng/µL × 10µL) was then added and the samples

168 incubated at room temperature for 6 to 8 hours. Peptides in gel spots were extracted

169 by 1% trifluoroacetic acid in 50% acetonitrile (ACN), and finally, the digested

170 peptides were condensed in 0.1% formic acid before MS analysis.

171 *2.4. Liquid chromatography and Electrospray Mass Spectrometry*

172 The mass spectrometer used for ESI-MS/MS was an ion trap mass spectrometer

173 (HCTultra PTM discovery system, Bruker Daltonik GmbH, Bremen, Germany)

174 operated in positive ion mode via a nanospray source. An Ultimate 3000 nanoHPLC

175 system (Dionex, Sunnyvale, CA) was used for the ESI experiments. The peptide

176 samples were concentrated on a C18 PepMap trapping column (300-µm

177 inner-diameter x 5mm, LC packing, Dionex, Sunnyvale, CA) and then separated on a

178 C18 PepMap column (75-µm inner-diameter x 150mm, LC packing, Dionex,

179 Sunnyvale, CA) with gradient conditions from 3-40% acetonitrile in 0.08% formic

180 acid at a flow rate of 200nL/min. Precursor selection was set as 350-1500m/z.

181 Collision induced dissociation fragmented the isolated top four abundant ions. The

182 generated MS spectra were searched against the chick International Protein Index

183 database (version 3.81) for protein identification via the Mascot search engine. The

184 processing of the raw individual MS data was conducted, using WarpLC 1.2

185 Software (Bruker Daltonik GmbH, Bremen, Germany), by calculating the relative

186   intensities of the extracted ion chromatograms, to obtain ratios of the abundance of

187   peptides and proteins (Light vs. Heavy).

188   *2.5. Mass Spectrometry settings for ICPL*

189   In quantitative experiments, the following search parameters were applied: a)

190   mass tolerance: 1.2 Da for peptide tolerance and 0.5 Da for MS/MS, respectively, b)

191   In data processing for protein identification without labeling, K (lysine), R (arginine),

192   D (aspartic acid) and E (glutamic acid) were set as the cleavage sites, while in data

193   processing for protein quantification with labeling, only R, D and E were set as

194   cleavage sites as K was labeled by isobaric tags and protected from trypsin cleavage.

195   One missed cleavage was allowed, c) charge states: 2+ and 3+, d) taxonomy was set

196   to Metazoa (Animals), e) fixed modification: carbamidomethylation of cysteine and

197   ICPL modifications of N-terminus and lysine residues, f) variable modification:

198   oxidation of methionine for protein identification, g) retention time window limited to

199   40 seconds.

200   *2.6. Validation of differentially regulated proteins by MRM-HR*

201   Targeted proteins with significant changes revealed in the discovery-based MS

202   were further validated by MRM-HR. Apart from their biological relevance, proteins

203   of interest were filtered with the following criteria for quality check: amino acid

204   length between 8-25 units, and unique peptide sequence, excluding peptides with

205   modifications. The MRM-HR data were analyzed with Skyline and MultiQuant

206   (version 3.03). The raw data were searched against the corresponding protein FASTA

207   sequence and matched with the previously acquired spectral library. After sample

208   preparation and digestion, as described above, each retinal sample was injected

209   individually to a TripleTOF 6600+ MS (Sciex, US). They were separated in a

210   120-minute effective gradient. Peptides of retinal samples (2μg in 4μL 0.1% formic

211   acid) were loaded on a trap column (C18, 200μm × 0.5mm) for 15 minutes at a speed

212 of 2 µl/min, then separated on a nano-LC column (75µm x 15cm, ChromXP C18, 3µm,

213 120Å) using an Ekisgent 415 nano-LC system. The LC separation was performed

214 under 300nL/min using mobile phase A (0.1% formic acid in 5% ACN) and B (0.1%

215 formic acid in 98% ACN) with the following gradient: 0-1min, 5%B; 1-91min,

216 5-20%B, 91-95 min, 20-35%B; 95-101min, 35-80%B, 101-111 min, 80%B, 111-113

217 min, 80-5%B; and 113-130 min, 5%B. The overall experimental workflow is shown

218 in Figure 1.

219
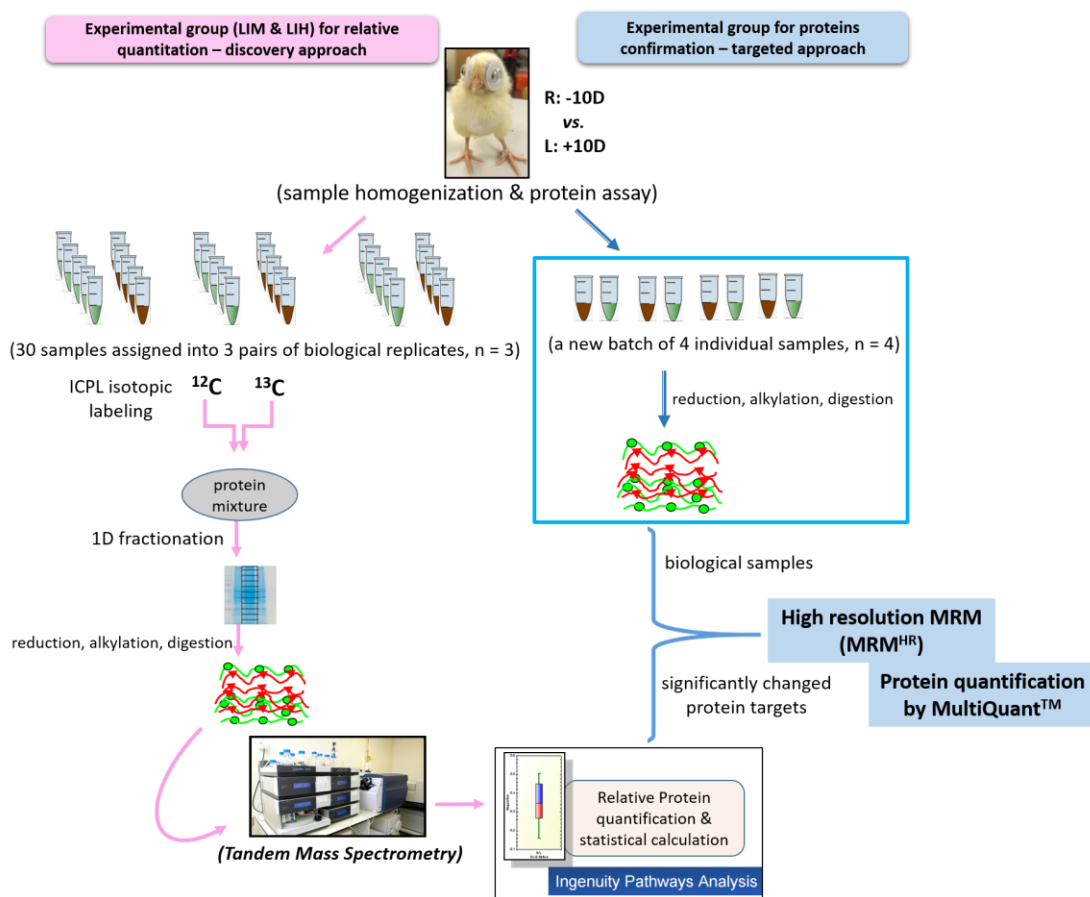
220

221 Figure 1. The experimental workflow of protein quantitation and validation in
222 ametropic chick retina, including the establishment of the chick model, sample
223 assignment, the technique applied, and data analysis.

224

225 *2.7. Data analysis*

226   Data was presented as mean value and standard deviation (mean ± SD). Each

227   discovery experiment at two time points was performed in triplicate (n = 3).

228   Criteria for protein identification (at least two top-ranking peptides hit) and

229   quantification ($p < 0.05$ using Student's paired t-test and average fold change

230   beyond 0.68 and 1.47) were the same as previously reported [19]. For MRM-HR

231   analysis, MultiQuant software 2.0 was used for calculation of relative abundance of

232   targeted peptides. The protein fold-change was calculated as an average of the

233   corresponding of individual peptides. Significant protein targets were exported to

234   the Ingenuity Pathway Analysis (IPA, Ingenuity Systems, Mountain View, CA) to

235   obtain a more integrated view of possible connections.

236

237   **3. Results**

238   *3.1. Biometric measurements after lens wear for 3 and 7 days*

239   As observed in an earlier study[19], chick eyes were found to be mildly

240   hyperopic at d0 (+4.00 ± 0.79D). There was no significant difference between any of

241   the values for right and left eyes, including refraction, axial length (AL), vitreous

242   chamber depth (VCD), and choroidal thickness (paired t-test, $p > 0.05$). After -10D

243   lens wear, the right eyes showed significant myopic shift. The refractive statuses were

244   -6.00 ± 1.82D at d3 (lens wear for 3 days) and -9.00 ± 2.10 at d7 (lens wear for 7 days)

245   with longer AL of 8.82 ± 0.21 mm and 9.14 ± 0.21 mm, respectively. In contrast,

246   hyperopia was induced by +10D lens wear on the contralateral eyes. The degree of

247   hyperopia was 9.25 ± 2.11D (d3) and 10.75± 2.16D (d7), respectively, accompanied

248   with shorter AL (8.10 ± 0.14 mm at d3 and 8.12 ± 0.16 mm at d7). Changes of VCD

249   contributed most to the changes of AL in both myopic and hyperopic eyes at both time

250   points. In contrast, the directions of changes in choroidal thickness were opposite to

251   the directions of VCD and AL, which became thicker in hyperopic and thinner in

252   myopic eyes as expected (Figure 2).

253

254

255
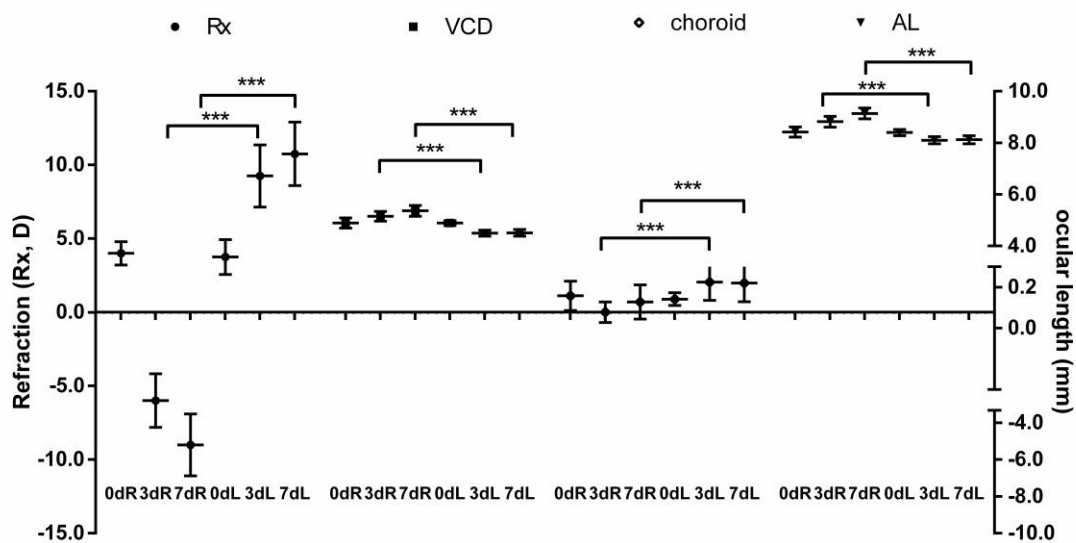
Figure 2. Refractive errors (Rx, left y-axis), axial length (AL, right y-axis), VCD
(right y-axis) and choroid thickness (right y-axis) before (0d) and after lens wear for 3
(3d) and 7 days (7d). Right (R) eyes wore -10D lenses while left (L) eye wore +10D
lenses. The refractive errors and three ocular components were significantly changed
between right and left eyes after lens wear (paired t-test, *** indicates $p < 0.05$ using
paired t-test, n = 15).

262   *3.2. Retinal protein identification in normal 7-day old chicks and quantification*

263   *after lens wear for 3 and 7 days*

264   A total of 1021 unique proteins in retinal tissue of normally raised 7-day old

265   chicks were identified as the chick retinal protein database (supplementary

266   information S1). The online PANTHER Gene list bioinformatics platform was used to

267   classify all identified proteins based on their biological process (BP), molecular

268   function (MF), and cellular component (CC). In terms of their involved BP, identified

269   proteins were mainly distributed in metabolic process (35.9%), cellular process

270   (18.1%) and localization (12.3%). In addition, the overwhelming majority of proteins

271   involved in metabolic processes belonged to primary metabolic processes (77.3%). In

272   the MF category, catalytic activity (40.4% belonging to hydrolases), binding (protein

273   binding: 44.5%; nucleic acid binding: 43.8%), and structural molecule activity were

274   the predominant three groups, accounting for 83% of all proteins in this category.

275   When classified by their CC, the majority of identified proteins were observed to be

276   located in cell structure (39.3%), macromolecular complexes (26.9%), and organelles

277   (26.5%). Only 0.7% of proteins in the retina were located in the extracellular region

278   (Figure 3).

279

280
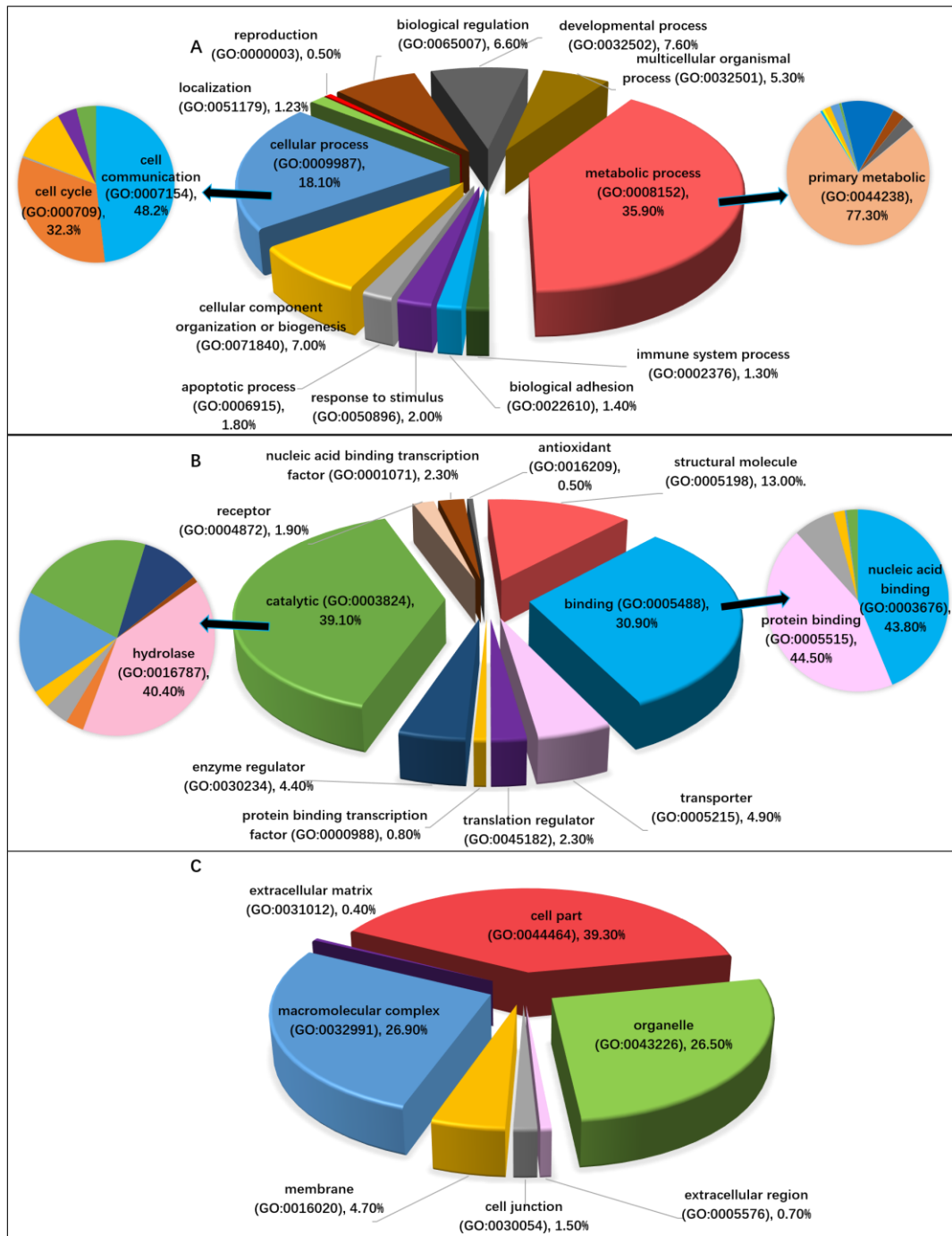
Figure 3. Pie chart showing the categories as a percentage of retinal proteins identified by tandem MS based on biological process, molecular function and cellular component using PANTHER classification system.

284

According to our preset criteria for quantitative analysis at a significant level ($p < 0.05$), a list of differentially regulated proteins present after two kinds of lens inducements for 3 and 7 days were detected by ICPL coupled to tandem MS. In the

288 myopic retina relative to the hyperopic (LIM/LIH), a total of six proteins were

289 significantly up-regulated: alpha-enolase; L-lactate dehydrogenase A chain (LDHA);

290 glutathione S-transferase (GSTM2); pyruvate kinase muscle isozyme (PKM2);

291 vimentin; and serine/threonine protein phosphatase. Three other proteins,

292 interphotoreceptor retinoid binding protein (IRBP); peroxiredoxin-6; and

293 glyceraldehyde-3-phosphate dehydrogenase, were significantly down-regulated. The

294 significantly changed proteins with their basic information from the PANTHER

295 online system [21] and UniProt [22] are shown in Table 1. The peptide information

296 for identification and protein regulation data including p-values are shown in

297 supplementary file S2.

298

299 Table 1. Basic information including their molecular function, cellular component,
300 and biological process of significantly regulated retinal proteins were listed. Red color
301 denotes proteins with significant upregulation (FC > 1.47), while blue color denotes
302 proteins with significant downregulation (FC < 0.68, LIM/LIH, *** indicates p < 0.05
303 using paired t-test, n = 3).

304

| Protein name	Accession number	MW (kDa)	pI	3d(-/+)	7d(-/+)	Molecular function	Cellular component	Biological process
peroxiredoxin-6	IPI00577013	25.1	5.63	0.65±0.12 ***	0.58±0.14 ***	antioxidant hydrolase peroxiredoxin	cytoplasm, cytoplasmic vesicle, lysosome	lipid degradation metabolism
GSTM2	IPI00580166	26.0	7.63	0.95±0.14	1.59±0.19 ***	transferase/glutathione transferase activity	cytoplasm	metabolic process
PKM	IPI00574064	58.4	7.96	1.56±0.13 ***	1.06±0.24	kinase, transferase	cytoplasm	carbohydrate metabolic glycolytic small molecule metabolic process
Vimentin	IPI00596934	53.2	4.94	1.59±0.28	1.61±0.49	structural molecule activity	cell projection/ intermediate filament	cellular component morphogenesis; cellular process
Alpha-enolase	IPI00575584	47.6	6.16	1.49±0.17 ***	1.21±0.10	magnesium ion binding, phosphopyruvate hydratase	cytoplasm phosphopyruvate hydratase complex	glycolysis gluconeogenesis carbohydrate metabolic small molecule metabolism
IRBP	IPI00607535	136.8	5.30	0.57±0.10 ***	0.59±0.16 ***	peptidase receptor	extracellular space	proteolysis
Serine/threonine protein phosphatase	IPI00576336	37.7	6.13	1.54±0.31	1.42±0.32	phosphoprotein phosphatase, calcium ion binding	cytoplasm	carbohydrate metabolism cell cycle/division glycogen metabolism
LDHA	IPI00584727	36.8	8.78	1.54±0.22 ***	1.45±0.10 ***	oxidoredutase	cytoplasm	glycolysis pyruvate metabolic process
GAPDH	IPI00594653	35.9	9.40	0.62±0.15 ***	1.42±0.42	oxidoreductase	cytoplasm, cytoskeleton	apoptosis; glycolysis

305

306

307 All differentially regulated protein candidates from discovery-based proteomics

308 were analyzed using Ingenuity Pathways Analysis [23]. The generated network

309   confirmed that all were located in the cytoplasm except IRBP, with maximum

310   connections to beta-estradiol and 3,5-diiodothyronine (Figure 4). In addition, insulin

311   in extracellular spaces was identified as an interactive pathway with the inputted

312   proteins. Further, glycolysis I and gluconeogenesis I canonical pathways were shown

313   to be the top two associated canonical pathways.

314
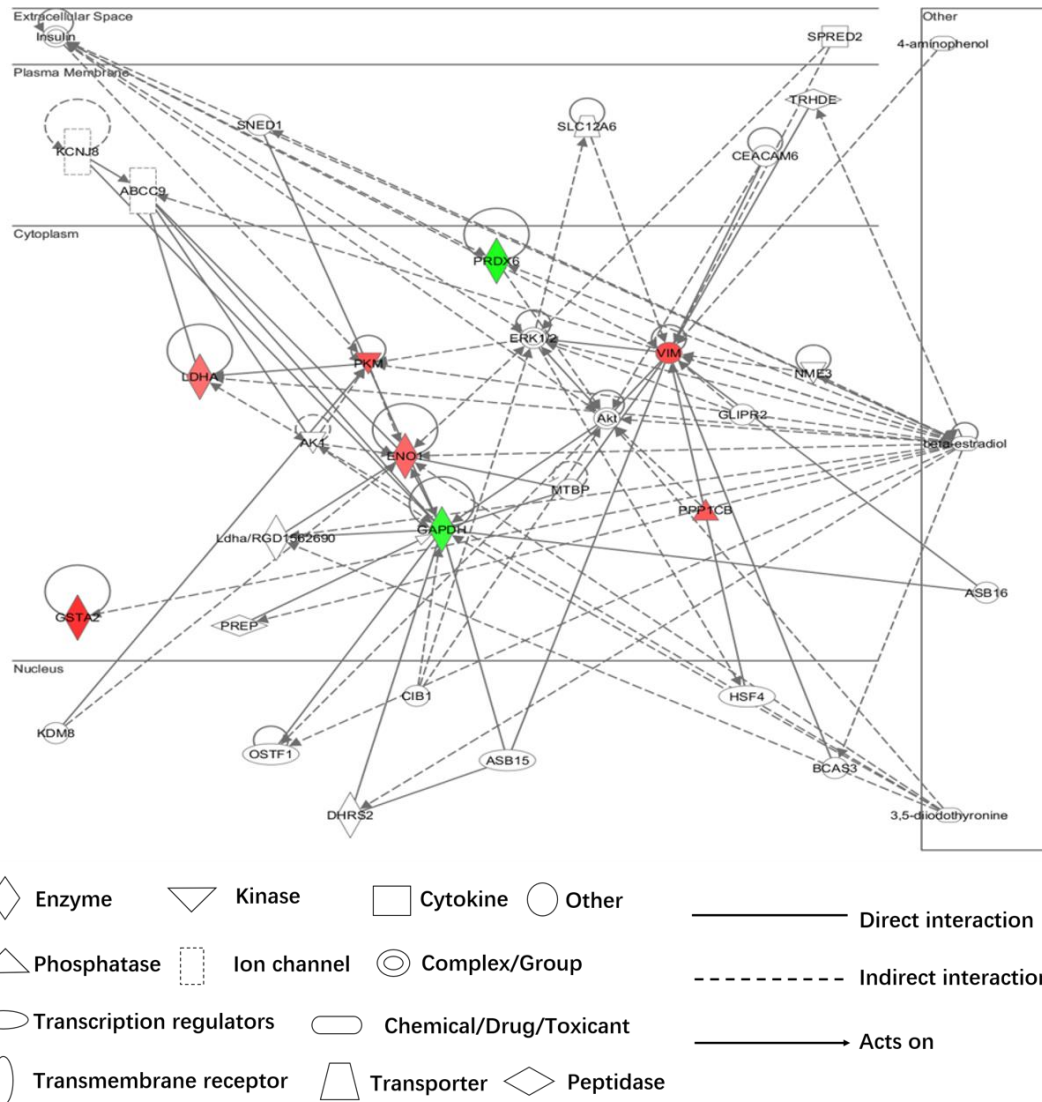
315   Figure 4. A protein-protein interactive network was generated by IPA using the
316   differentially regulated proteins during ocular growth (LIM/LIH). The meanings of
317   symbols and lines in the network are shown in the figure. The protein names of gene
318   symbols are as follows: GSTA2: glutathione S-transferase 2, ENO1: alpha-enolase,
319   LDHA: interphotoreceptor retinoid binding protein, VIM: vimentin, PRDX6:
320   peroxiredoxin-6, PKM: pyruvate kinase muscle isozyme, PPP1CB: serine/threonine
321   protein phosphatase, GAPDH: glyceraldehyde 3-phosphate dehydrogenase.

322

3.3. Confirmation by high-resolution MRM-HR

Table 2. MRM-HR results of five proteins in the ametropic chick retina. The information including sequence, transition and relative ratio for each used peptide was shown. Ratios of proteins were calculated from relative ratios of peptides. Red color denotes significant upregulation while blue color denotes significant downregulation (LIM/LIH, paired t-test, *** indicates $p < 0.05$, n = 12).

Protein name	Protein ratio (-10D/+10D)	Peptide sequence	Transition	Peptide ratio (-10D/+10D)
Vimentin	1.73±0.40***	KVESLQEEIVFLK	2y11, 2b9, 2b1	1.49±0.37
		QIQSLTC[CAM]EVDALK	2y8, 2y10, 2y11	1.52±0.24
		VEVERDNLADDIMR	3y5, 3y6, 3b7	2.19±0.35
GSTM2	1.60±0.34***	LGLDFPNLPYLIDGDVK	3y6, 3y8, 3y9	1.88±0.22
		LLLEYTETPYQER	2y8, 2y9, 2y10	1.69±0.25
		VDVLENHLMDLR	3b2, 3y8, 3y2	1.22±0.12
IRBP	0.52±0.04***	FSFHTNVFENNIGYLR	3y4, 3y7, 3b7	0.56±0.19
		DSIPGILPK	2y2, 2y5, 2y6	0.52±0.16
		LVDTDAMIIDMR	3y2, 3y4, 3y5	0.48±0.16
ApoAI	0.67±0.03***	LISFLDELQK	2y6	0.62±0.24
		LISFLDELQK	2y5	0.71±0.36
		LISFLDELQK	2y8	0.65±0.26
Peroxiredoxin-6	0.94±0.13	LSILYPATTGR	2y6, 2y7, 2y8	0.95±0.13
		MIALSIDSVPDHLAWSK	3y5, 3y8, 3y11	0.95±0.11
		VVFIFGPDK	2y4, 2y5, 2y7	0.92±0.16

329

Due to the low abundance of the targeted retinal proteins and lack of specific antibodies for chicken, western blot confirmation remains a challenge in confirming the relative abundance of proteins found by discovery-based proteomics. We applied a high-resolution Multiple Reaction Monitoring (MRM-HR) MS for confirming the fold changes present in four discovered proteins with evident alterations (vimentin, GSTM2 IRBP, and peroxiredoxin-6) in the chick retina at d7. This new approach using a Triple-ToF MS was proven to be useful in detecting regulated retinal protein changes during the emmetropization process in our recent study [24]. The experimental parameters for data acquisition are attached in supplementary file S3. A

339   new batch of chicks (n = 4) wearing -10D lenses on their right eyes and +10D lenses

340   on the left were hatched to harvest retinal samples for MRM-HR confirmation. The

341   targeted proteomics at transitional levels indicated that change in peroxiredoxin-6 was

342   not statistically significant ($p > 0.05$), although its relative abundance was shown to

343   be decreased as found by discovery-based proteomics. The three other proteins were

344   significantly changed ($p < 0.05$) in the same direction as suggested using ICPL

345   labeled profiling approach. In addition, ApoA1, a protein frequently reported as a

346   target in ametropia, including in our previous quantitative study in ametropic vitreous,

347   was shown to be down-regulated by MRM-HR in the retina (Table 2).

348

349   **4. Discussion**

350   Research on the vitreous-retina complex has merit in studying vitreoretinal

351   diseases. Compared to our previous protein identification in vitreous humor using

352   normally raised 7-day old chicks [19], both common and unique features in these

353   adjacent tissues were revealed in the current study. Classified by gene function, the

354   overall profile in chick vitreous and retina was surprisingly quite similar in terms of

355   BP and MF, but the percentage involved in CC was different. More vitreous proteins

356   located in extracellular regions and the extracellular matrix were identified. This may

357   indicate the sources of proteins in the two adjacent tissues differed. Furthermore, it

358   was possible to extract more proteins from extracellular regions/matrix due to the

359   gel-like substance of vitreous. However, although additional proteins were identified

360   by the aid of the advanced technology, the classification of the chick retinal proteome

361   reported in this study was almost the same as in the human retina for all three

362   functional categories, namely BP, MF, and CC [25], which supports the relevance of

363   use of the young chick as a human myopia model.

364   With respect to protein alterations in vitreous and retina tissues, different

365 changes were observed. Firstly, significantly changed protein biomarkers were mainly

366 of cytoplasmic origin in the retina, whilst they originated from extracellular regions in

367 vitreous materials. This finding was reasonable as cytoplasm contains enzymes to

368 catalyze various reactions and is known to be the main site for most cellular activities

369 to take place. It was an expected finding as it is well-recognized that biochemical and

370 metabolic activities in the retina are vigorous. Secondly, a number of glycolytic

371 enzymes were found to be up-regulated in the myopic retina, including LDHA, PKM2,

372 and alpha-enolase. Pathway analysis by IPA also indicated the involvement of

373 glycolysis and gluconeogenesis in the retina during myopia development. The

374 relationship of glycolysis to myopia has previously been reported in the myopic

375 mouse retina and myopic/recovery tree shrew sclera [14, 18]. The findings of this

376 study infer a hypoxic environment may be involved in the progression of myopia. The

377 association of myopia to glycolysis and hypoxia will be discussed further below.

378 Finally, this study provides further evidence of the participation of retinal protein

379 targets in various metabolic processes during myopia development. These included

380 enzymes involved in the metabolism of lipids (peroxiredoxin-6), pyruvate (lactate

381 dehydrogenase), glycogen (serine/threonine phosphatase), carbohydrates

382 (serine/threonine phosphatase and pyruvate kinase), and small molecule (pyruvate

383 kinase) metabolism. This association has also been reported in the retina of a

384 form-deprived myopia (FDM) model[26] and in scleral tissue [27].

385   Oxygen supply and consumption play a critical role in normal growth, especially

386 in the retina, the most metabolically active tissue [28]. It was well known that retinal

387 nutrition and oxygen are supplied by retinal arteries and choroidal vessels. Thinning

388 of the choroid during myopia development results in a decreased supply of nutrition

389 and oxygen. At the same time, exaggerated ocular growth leads to a higher demand

390 for oxygen and nutrition from the retinal source. Thus, the myopic eye could be prone

391 to hypoxia. In normal growth, aerobic oxidation is the major pathway to generate and

392 provide energy, while the main function of glycolysis is to provide energy quickly.

393 Therefore, our findings support the hypothesis of a hypoxic environment existing in

394 the myopic chick as indicated by the up-regulation of glycolysis related proteins. A

395 decline of aerobic glycolysis and an energy-conserving metabolism in myopia has

396 been previously demonstrated [26]. Furthermore, a comprehensive study reported the

397 presence of hypoxic conditions in the myopic sclera and the effectiveness of using

398 anti-hypoxic drugs in the reduction of myopia [29]. This study's findings, confirming

399 the likelihood of a hypoxic environment in the myopic eye, indicate that a therapeutic

400 approach for myopia via regulating hypoxia or oxygen supply in the posterior ocular

401 tissues is worthy of further study.

402 Except for the differences mentioned above, there were similar findings

403 regarding protein alterations in the adjacent tissues and the results agreed with

404 previous studies. The magnitude of all changes in relative abundance were mild or

405 moderate (less than 2.0-fold change), no matter whether the changes were comparison

406 of the myopic eye to control, contralateral, or hyperopic eyes [30]. It also appeared

407 more proteins were altered after a shorter period (3 days) of lens wear than over a

408 longer period (7 days) when the eyes were approaching full compensation of the

409 -10D/+10D treatment. Therefore, it was suggested there is a rapid initial response in

410 the eye to an external defocus signal [19]. In addition, several common protein

411 biomarkers were shared between the two time points, which are discussed in further

412 detail below. Taken together, the current study and earlier quantitative studies provide

413 a novel and sensitive alternative to validate relative changes in ocular proteins [31].

414 The integrated proteomics methodology has been successfully applied and

415 demonstrated as a useful tool for providing new insights for protein interactions in

416 various ocular conditions in our previous studies [24, 32].

417   Of the differentially regulated proteins identified in the myopic retina, Apo A1

418   was one of the biomarkers related to ocular changes. Since the first report in 2006,

419   it has frequently been identified as having a significant role in myopia development

420   [9, 14, 15]. Bertrand et al showed that a PPAR-alpha agonist could affect HDL

421   metabolism leading to an increase in levels of Apo A1. Vitamin D-binding protein

422   was proposed to be involved in the STOP pathway of Apo A1 [33]. Additionally,

423   Apo A1 levels in chick retina could be elevated by cyclic adenosine

424   monophosphate (cAMP), helping to inhibit the development of myopia [34]. Apo

425   A1 mRNA in chick choroid was increased following treatment with retinoic acid

426   [15]. Summers et al further identified Apo A1 as a retinoic acid-binding protein. In

427   our studies, Apo A1 was down-regulated in the myopic retina, but was up-regulated

428   in vitreous in relative myopic over relative hyperopic eyes [19]. This may be

429   explained by the dynamic movement of Apo A1 between the vitreous and the retina,

430   but this possible mechanism requires further studies.

431   IRBP may be another valuable target involved in myopia development. IRBP

432   is a glycoprotein present in the extracellular space between the photoreceptors and

433   the retinal pigment epithelium. It is critical for vision to maintain photoreceptors

434   and the visual cycle in response to the external visual stimuli [35]. IRBP-deficient

435   mice displayed an increasing trend to develop myopia and exaggerated eye growth

436   [36, 37]. A clinical study also showed mutations in RBP3 (encoding IRBP) could

437   induce the development of high myopia and retinal dystrophy in children [38].

438   These studies are in accordance with our current finding, which revealed that IRBP

439   was decreased in myopic chicks. One possible mechanism may be again mediated

440   by retinoic acid, which was suggested to signal the direction of ocular elongation

441   [39], as the transfer of all-trans-retinol between photoreceptors and the retinal

442   pigment epithelium is mediated by IRBP [35, 40]. As the increased level of retinoic

443 acid mediated the onset and development of myopia, we believe further studies to

444 examine synergistic changes of retinal retinoic acid, IRBP, and also Apo A1 in

445 myopia development are warranted.

446 Another target of interest is vimentin, a static structural protein. It is thought to

447 play a critical role in a number of signaling pathways and essential cellular

448 processes [41]. It was reported to be up-regulated in myopic retinas of chick models

449 [9]. Up-regulation of retinal vimentin in FDM guinea pigs was also observed in our

450 previous work [42]. In addition, vimentin was reported to be decreased in myopic

451 and recovery sclera of a tree shrew model [14]. Its up-regulation in the current

452 study further confirmed the significance of vimentin in the myopic chick retina,

453 although little information has been reported on the role of vimentin in ocular

454 growth.

455 Other identified proteins included GSTM2, Peroxiredoxin-6 (Prdx6), PKM2,

456 and LDHA, although down-regulation of Prdx6 in discovery was not validated by

457 MRM-HR, possibly due to variation of quantification and instrumental sensitivity.

458 These four proteins are all related to oxidative processes. Two of the proteins

459 (PKM2 and LDHA) are also related to glycolysis, as discussed above. GSTM2

460 plays a crucial role in the regulation of oxidative stress-mediated cellular signaling

461 process [43]. Prdx6-targeted mutant mice showed reduced survival time, increased

462 tissue damage, and higher protein oxidation levels [44]. Increased abundance of

463 Prdx6 protein in mice lungs can significantly protect against hyperoxic injury and

464 delay death [45]. Increased regulation of PKM2 suggested enhanced glycolysis [46].

465 LDHA can reduce pyruvate, the major product of glycolysis, to lactate, when

466 limited amounts of oxygen are available. Damage to the retina by oxidative stress

467 has been reported to be associated with hypoxia [47]. Collectively, alterations in

468 levels of these four proteins all indicate the likelihood of hypoxia, which provided

469   proteomics support to a recent theory of altered oxidative stress during myopia

470   development [17]. As suggested above, hypoxia management in myopia control

471   may be an important focus of further studies.

472   In addition to discussion of the roles of the individual proteins, interpretation

473   of changes in myopia was further explored using pathway analysis supported by

474   Ingenuity Pathway Analysis (IPA) bioinformatics. The changes of our differentially

475   regulated proteins are found to be related to the insulin pathway, 3,

476   5-diiodothyronine (3,5-T2), and beta-estradiol. Insulin related metabolism has long

477   been a classic pathway suggested in myopia. Intravitreal insulin was shown to be a

478   powerful stimulator of axial growth in the chicken myopia model [48, 49]. Also, it

479   was known that high carbohydrate diets may worsen refractive errors during early

480   growth and later development and be related to insulin levels [50]. Further, the

481   prevalence of myopia was found to be higher in diabetic than non-diabetic patients,

482   supporting a relationship between altered insulin metabolism and myopia

483   development [51]. Insulin resistance (inability to stimulate glucose uptake into cells)

484   is the major mechanism in Type 2 diabetes, by blocking the binding of insulin to its

485   receptor [52]. Increased resistance to insulin in people of Asian descent may

486   explain the higher prevalence of myopia in Asian countries [53]. The linkage of the

487   role of insulin with changes in various retinal protein levels found by the pathway

488   analysis further strengthens the hypothesis of a relationship of myopia to insulin

489   metabolism.

490   3, 5-diiodothyronine is an active thyroid hormone and belongs to the family of

491   iodine-dependent thyroid hormones. It has a rapid effect on energy balance, by

492   increasing oxygen consumption and affecting the activity of enzymes involved in

493   energy metabolism [54, 55]. Thyroid-stimulating hormone also has an interaction

494   with insulin in regulating thyroid growth [56]. Thus, 3, 5-diiodothyronine may

495   participate in energy metabolism and the insulin pathway. The proposed similar

496   pathways highlighted by IPA may suggest shared molecular functions of our

497   identified proteins. Another observed pathway identified by IPA was beta-estradiol,

498   the primary female sex hormone in the maintenance of female reproductive tissues.

499   Clinical studies in the Asian population have suggested potential involvement of

500   sex hormones in myopia [57, 58]. However, gender-specific effects were not

501   considered in the design of the current study as the chicks were randomly selected

502   and sex of chicks in the groups was not recorded. More specific studies should take

503   gender into consideration and analyze the effect of beta-estradiol in myopia.

504

505   **5. Conclusions**

506   Despite the limited tissue size of ocular samples, advancements in proteomics

507   strategy, combining isotopic labeled profiling and targeted label free MRM-HR

508   quantification, provide a sensitive platform contributing to a more comprehensive

509   understanding of protein abundance during myopia development. The results in the

510   retina supplement our recent report of vitreous proteomics in chick myopia,

511   supporting the notion of myopia as a disorder of abnormal metabolism

512   accompanied by hypoxia conditions. Follow-up experiments can be performed to

513   alter the regulation of potential biomarkers or pathways to study possible

514   interventions for the control and treatment of myopia.

515

516   **Declaration of Competing Interest**

517   The authors have declared no conflict of interest.

518   **Appendix. Supplementary data**

519   Supplementary materials of the identified proteins in chick retina using

520   ESI-MS/MS can be found at supplementary file S1. List of peptides contributing to

the identification of differentially expressed proteins with their respective

regulation data at the two time points is attached in supplementary data S2. The

experimental parameters for the data acquisition of MRM-HR are shown in

supplementary file S3.

Supplementary data to this article can be found online at https://
doi.org/10.1016/j.jprot.2020.103684.

References

[1] Y. Ikuno, Overview of the Complications of High Myopia, Retina 37(12) (2017) 2347-2351.

[2] B.A. Holden, T.R. Fricke, D.A. Wilson, M. Jong, K.S. Naidoo, P. Sankaridurg, T.Y. Wong, T.J. Naduvilath, S. Resnikoff, Global Prevalence of Myopia and High Myopia and Temporal Trends from 2000 through 2050, Ophthalmology 123(5) (2016) 1036-1042.

[3] M. Chen, A. Wu, L. Zhang, W. Wang, X. Chen, X. Yu, K. Wang, The increasing prevalence of myopia and high myopia among high school students in Fenghua city, eastern China: a 15-year population-based survey, BMC Ophthalmol 18(1) (2018) 159.

[4] Y.P. Huang, A. Singh, L.J. Lai, The Prevalence and Severity of Myopia among Suburban Schoolchildren in Taiwan, Ann Acad Med Singapore 47(7) (2018) 253-259.

[5] S. Sensaki, C. Sabanayagam, P.K. Verkicharla, A. Awodele, K.H. Tan, A. Chia, S.M. Saw, An Ecologic Study of Trends in the Prevalence of Myopia in Chinese Adults in Singapore Born from the 1920s to 1980s, Ann Acad Med Singapore 46(6) (2017) 229-236.

[6] D.I. Flitcroft, Emmetropisation and the aetiology of refractive errors, Eye (Lond) 28(2) (2014) 169-179.

[7] D. Troilo, E.L. Smith, 3rd, D.L. Nickla, R. Ashby, A.V. Tkatchenko, L.A. Ostrin, T.J. Gawne, M.T. Pardue, J.A. Summers, C.S. Kee, F. Schroedl, S. Wahl, L. Jones, IMI - Report on Experimental Models of Emmetropization and Myopia, Invest Ophthalmol Vis Sci 60(3) (2019) M31-M88.

[8] I.G. Morgan, The biological basis of myopic refractive error, Clin Exp Optom 86(5) (2003) 276-288.

[9] E. Bertrand, C. Fritsch, S. Diether, G. Lambrou, D. Muller, F. Schaeffel, P. Schindler, K.L. Schmid, J. van Oostrum, H. Voshol, Identification of apolipoprotein

556   A-I as a "STOP" signal for myopia, Mol Cell Proteomics 5(11) (2006) 2158-2166.

557   [10] C.J. Wolsley, K.J. Saunders, G. Silvestri, R.S. Anderson, Investigation of changes
558   in the myopic retina using multifocal electroretinograms, optical coherence
559   tomography and peripheral resolution acuity, Vision Res 48(14) (2008) 1554-1561.

560   [11] N. Riddell, S.G. Crewther, Novel evidence for complement system activation in
561   chick myopia and hyperopia models: a meta-analysis of transcriptome datasets, Sci
562   Rep 7(1) (2017) 9719.

563   [12] N. Riddell, S.G. Crewther, Integrated Comparison of GWAS, Transcriptome, and
564   Proteomics Studies Highlights Similarities in the Biological Basis of Animal and
565   Human Myopia, Invest Ophthalmol Vis Sci 58(1) (2017) 660-669.

566   [13] T.C. Lam, K.K. Li, S.C. Lo, J.A. Guggenheim, C.H. To, A chick retinal proteome
567   database and differential retinal protein expressions during early ocular development,
568   J Proteome Res 5(4) (2006) 771-784.

569   [14] M.R. Frost, T.T. Norton, Alterations in protein expression in tree shrew sclera
570   during development of lens-induced myopia and recovery, Invest Ophthalmol Vis Sci
571   53(1) (2012) 322-336.

572   [15] J.A. Summers, A.R. Harper, C.L. Feasley, H. Van-Der-Wel, J.N. Byrum, M.
573   Hermann, C.M. West, Identification of Apolipoprotein A-I as a Retinoic Acid-binding
574   Protein in the Eye, J Biol Chem 291(36) (2016) 18991-19005.

575   [16] N. Riddell, L. Giummarra, N.E. Hall, S.G. Crewther, Bidirectional Expression of
576   Metabolic, Structural, and Immune Pathways in Early Myopia and Hyperopia, Front
577   Neurosci 10 (2016) 390.

578   [17] B.M. Francisco, M. Salvador, N. Amparo, Oxidative stress in myopia, Oxid Med
579   Cell Longev 2015 (2015) 750637.

580   [18] V.A. Barathi, S.S. Chaurasia, M. Poidinger, S.K. Koh, D. Tian, C. Ho, P.M.
581   Iuvone, R.W. Beuerman, L. Zhou, Involvement of GABA transporters in
582   atropine-treated myopic retina as revealed by iTRAQ quantitative proteomics, J
583   Proteome Res 13(11) (2014) 4647-4658.

584   [19] F.J. Yu, T.C. Lam, L.Q. Liu, R.K. Chun, J.K. Cheung, K.K. Li, C.H. To,
585   Isotope-coded protein label based quantitative proteomic analysis reveals significant
586   up-regulation of apolipoprotein A1 and ovotransferrin in the myopic chick vitreous,
587   Sci Rep 7(1) (2017) 12649.

588   [20] J.M. Skeie, V.B. Mahajan, Proteomic interactions in the mouse vitreous-retina
589   complex, PLoS One 8(11) (2013) e82140.

590   [21] H. Mi, A. Muruganujan, J.T. Casagrande, P.D. Thomas, Large-scale gene
591   function analysis with the PANTHER classification system, Nat Protoc 8(8) (2013)
592   1551-1566.

593   [22] C. The UniProt, UniProt: the universal protein knowledgebase, Nucleic Acids

594 Res 45(D1) (2017) D158-D169.

595 [23] A. Kramer, J. Green, J. Pollard, Jr., S. Tugendreich, Causal analysis approaches
596 in Ingenuity Pathway Analysis, Bioinformatics 30(4) (2014) 523-530.

597 [24] S.W. Shan, D.Y. Tse, B. Zuo, C.H. To, Q. Liu, S.A. McFadden, R.K. Chun, J.
598 Bian, K.K. Li, T.C. Lam, Integrated SWATH-based and targeted-based proteomics
599 provide insights into the retinal emmetropization process in guinea pig, J Proteomics
600 (2018).

601 [25] G. Velez, D.A. Machlab, P.H. Tang, Y. Sun, S.H. Tsang, A.G. Bassuk, V.B.
602 Mahajan, Proteomic analysis of the human retina reveals region-specific
603 susceptibilities to metabolic- and oxidative stress-related diseases, PLoS One 13(2)
604 (2018) e0193250.

605 [26] J. Yang, P.S. Reinach, S. Zhang, M. Pan, W. Sun, B. Liu, F. Li, X. Li, A. Zhao, T.
606 Chen, W. Jia, J. Qu, X. Zhou, Changes in retinal metabolic profiles associated with
607 form deprivation myopia development in guinea pigs, Sci Rep 7(1) (2017) 2777.

608 [27] N.A. McBrien, Regulation of scleral metabolism in myopia and the role of
609 transforming growth factor-beta, Exp Eye Res 114 (2013) 128-140.

610 [28] K. Kooragayala, N. Gotoh, T. Cogliati, J. Nellissery, T.R. Kaden, S. French, R.
611 Balaban, W. Li, R. Covian, A. Swaroop, Quantification of Oxygen Consumption in
612 Retina Ex Vivo Demonstrates Limited Reserve Capacity of Photoreceptor
613 Mitochondria, Invest Ophthalmol Vis Sci 56(13) (2015) 8428-8436.

614 [29] H. Wu, W. Chen, F. Zhao, Q. Zhou, P.S. Reinach, L. Deng, L. Ma, S. Luo, N.
615 Srinivasalu, M. Pan, Y. Hu, X. Pei, J. Sun, R. Ren, Y. Xiong, Z. Zhou, S. Zhang, G.
616 Tian, J. Fang, L. Zhang, J. Lang, D. Wu, C. Zeng, J. Qu, X. Zhou, Scleral hypoxia is a
617 target for myopia control, Proc Natl Acad Sci U S A 115(30) (2018) E7091-E7100.

618 [30] R. Jostrup, W. Shen, J.T. Burrows, J.G. Sivak, B.J. McConkey, T.D. Singer,
619 Identification of myopia-related marker proteins in tilapia retinal, RPE, and choroidal
620 tissue following induced form deprivation, Curr Eye Res 34(11) (2009) 966-975.

621 [31] L. Tong, X.Y. Zhou, A. Jylha, U. Aapola, D.N. Liu, S.K. Koh, D. Tian, J. Quah,
622 H. Uusitalo, R.W. Beuerman, L. Zhou, Quantitation of 47 human tear proteins using
623 high resolution multiple reaction monitoring (HR-MRM) based-mass spectrometry, J
624 Proteomics 115 (2015) 36-48.

625 [32] S.W. Shan, C.W. Do, T.C. Lam, R.P.W. Kong, K.K. Li, K.M. Chun, W.D. Stamer,
626 C.H. To, New Insight of Common Regulatory Pathways in Human Trabecular
627 Meshwork Cells in Response to Dexamethasone and Prednisolone Using an
628 Integrated Quantitative Proteomics: SWATH and MRM-HR Mass Spectrometry, J
629 Proteome Res 16(10) (2017) 3753-3765.

630 [33] X. Duan, Q. Lu, P. Xue, H. Zhang, Z. Dong, F. Yang, N. Wang, Proteomic
631 analysis of aqueous humor from patients with myopia, Mol Vis 14 (2008) 370-377.

632   [34] R.K. Chun, S.W. Shan, T.C. Lam, C.L. Wong, K.K. Li, C.W. Do, C.H. To, Cyclic

633   Adenosine Monophosphate Activates Retinal Apolipoprotein A1 Expression and

634   Inhibits Myopic Eye Growth, Invest Ophthalmol Vis Sci 56(13) (2015) 8151-8157.

635   [35] M. Jin, S. Li, S. Nusinowitz, M. Lloyd, J. Hu, R.A. Radu, D. Bok, G.H. Travis,

636   The role of interphotoreceptor retinoid-binding protein on the translocation of visual

637   retinoids and function of cone photoreceptors, J Neurosci 29(5) (2009) 1486-1495.

638   [36] J. Wisard, A. Faulkner, M.A. Chrenek, T. Waxweiler, W. Waxweiler, C.

639   Donmoyer, G.I. Liou, C.M. Craft, G.F. Schmid, J.H. Boatright, M.T. Pardue, J.M.

640   Nickerson, Exaggerated eye growth in IRBP-deficient mice in early development,

641   Invest Ophthalmol Vis Sci 52(8) (2011) 5804-5811.

642   [37] S. Markand, N.L. Baskin, R. Chakraborty, E. Landis, S.A. Wetzstein, K.J.

643   Donaldson, P. Priyadarshani, S.E. Alderson, C.S. Sidhu, J.H. Boatright, P.M. Iuvone,

644   M.T. Pardue, J.M. Nickerson, IRBP deficiency permits precocious ocular

645   development and myopia, Mol Vis 22 (2016) 1291-1308.

646   [38] G. Arno, S. Hull, A.G. Robson, G.E. Holder, M.E. Cheetham, A.R. Webster, V.

647   Plagnol, A.T. Moore, Lack of Interphotoreceptor Retinoid Binding Protein Caused by

648   Homozygous Mutation of RBP3 Is Associated With High Myopia and Retinal

649   Dystrophy, Invest Ophthalmol Vis Sci 56(4) (2015) 2358-2365.

650   [39] S.A. McFadden, M.H. Howlett, J.R. Mertz, Retinoic acid signals the direction of

651   ocular elongation in the guinea pig eye, Vision Res 44(7) (2004) 643-653.

652   [40] M. Garcia-Ramirez, C. Hernandez, M. Villarroel, F. Canals, M.A. Alonso, R.

653   Fortuny, L. Masmiquel, A. Navarro, J. Garcia-Arumi, R. Simo, Interphotoreceptor

654   retinoid-binding protein (IRBP) is downregulated at early stages of diabetic

655   retinopathy, Diabetologia 52(12) (2009) 2633-2641.

656   [41] K.M. Ridge, D. Shumaker, A. Robert, C. Hookway, V.I. Gelfand, P.A. Janmey, J.

657   Lowery, M. Guo, D.A. Weitz, E. Kuczmarski, R.D. Goldman, Methods for

658   Determining the Cellular Functions of Vimentin Intermediate Filaments, Methods

659   Enzymol 568 (2016) 389-426.

660   [42] Q.L. Yi Wu, Chi Ho To, King-Kit Li, Rachel K.M. Chun, Jessica F.J. Yu and

661   Thomas C. Lam, Differential Retinal Protein Expressions During form Deprivation

662   Myopia in Albino Guinea Pigs, Current Proteomics 11 (2014) 37-47.

663   [43] Y.C. Awasthi, G.A. Ansari, S. Awasthi, Regulation of 4-hydroxynonenal mediated

664   signaling by glutathione S-transferases, Methods Enzymol 401 (2005) 379-407.

665   [44] X. Wang, S.A. Phelan, K. Forsman-Semb, E.F. Taylor, C. Petros, A. Brown, C.P.

666   Lerner, B. Paigen, Mice with targeted mutation of peroxiredoxin 6 develop normally

667   but are susceptible to oxidative stress, J Biol Chem 278(27) (2003) 25179-25190.

668   [45] Y. Wang, Y. Manevich, S.I. Feinstein, A.B. Fisher, Adenovirus-mediated transfer

669   of the 1-cys peroxiredoxin gene to mouse lung protects against hyperoxic injury, Am J

670   Physiol Lung Cell Mol Physiol 286(6) (2004) L1188-1193.

671   [46] H.R. Christofk, M.G. Vander Heiden, M.H. Harris, A. Ramanathan, R.E.
672   Gerszten, R. Wei, M.D. Fleming, S.L. Schreiber, L.C. Cantley, The M2 splice isoform
673   of pyruvate kinase is important for cancer metabolism and tumour growth, Nature
674   452(7184) (2008) 230-233.

675   [47] S.Y. Li, Z.J. Fu, A.C. Lo, Hypoxia-induced oxidative stress in ischemic
676   retinopathy, Oxid Med Cell Longev 2012 (2012) 426769.

677   [48] M.P. Feldkaemper, I. Neacsu, F. Schaeffel, Insulin acts as a powerful stimulator
678   of axial myopia in chicks, Invest Ophthalmol Vis Sci 50(1) (2009) 13-23.

679   [49] X. Zhu, J. Wallman, Opposite effects of glucagon and insulin on compensation
680   for spectacle lenses in chicks, Invest Ophthalmol Vis Sci 50(1) (2009) 24-36.

681   [50] L. Cordain, S.B. Eaton, J. Brand Miller, S. Lindeberg, C. Jensen, An evolutionary
682   analysis of the aetiology and pathogenesis of juvenile-onset myopia, Acta Ophthalmol
683   Scand 80(2) (2002) 125-135.

684   [51] N. Jacobsen, H. Jensen, H. Lund-Andersen, E. Goldschmidt, Is poor glycaemic
685   control in diabetic patients a risk factor of myopia?, Acta Ophthalmol 86(5) (2008)
686   510-514.

687   [52] J. Ye, Regulation of PPARgamma function by TNF-alpha, Biochem Biophys Res
688   Commun 374(3) (2008) 405-408.

689   [53] S. Ehtisham, N. Crabtree, P. Clark, N. Shaw, T. Barrett, Ethnic differences in
690   insulin resistance and body composition in United Kingdom adolescents, J Clin
691   Endocrinol Metab 90(7) (2005) 3963-3969.

692   [54] F. Goglia, The effects of 3,5-diiodothyronine on energy balance, Front Physiol 5
693   (2014) 528.

694   [55] A.S. Padron, R.A. Neto, T.U. Pantaleao, M.C. de Souza dos Santos, R.L. Araujo,
695   B.M. de Andrade, M. da Silva Leandro, J.P. de Castro, A.C. Ferreira, D.P. de Carvalho,
696   Administration of 3,5-diiodothyronine (3,5-T2) causes central hypothyroidism and
697   stimulates thyroid-sensitive tissues, J Endocrinol 221(3) (2014) 415-427.

698   [56] M.C. Eggo, L.K. Bachrach, G.N. Burrow, Interaction of TSH, insulin and
699   insulin-like growth factors in regulating thyroid growth and function, Growth Factors
700   2(2-3) (1990) 99-109.

701   [57] Z.T. Chen, I.J. Wang, Y.T. Liao, Y.F. Shih, L.L. Lin, Polymorphisms in
702   steroidogenesis genes, sex steroid levels, and high myopia in the Taiwanese
703   population, Mol Vis 17 (2011) 2297-2310.

704   [58] J.F. Gong, H.L. Xie, X.J. Mao, X.B. Zhu, Z.K. Xie, H.H. Yang, Y. Gao, X.F. Jin,
705   Y. Pan, F. Zhou, Relevant factors of estrogen changes of myopia in adolescent females,
706   Chin Med J (Engl) 128(5) (2015) 659-663.

707